Simulation of Piezoelectric Dome-Shaped-Diaphragm Acoustic Transducers

Cheol-Hyun Han* and Eun Sok Kim**

***Abstract*—This paper describes the simulation of a micromachined dome-shaped-diaphragm acoustic transducer built on a 1.5 μm thick silicon nitride diaphragm (2,000 μm in radius, with a circular clamped boundary on a silicon substrate) with electrodes and piezoelectric ZnO film in a silicon substrate. Finite element analysis with ANSYS 5.6 has been performed to analyze the static and dynamic behaviors of the transducer under both pressure and voltage loadings.**

***Index Terms*—MEMS, FEA, acoustic transducer, piezoelectric, dome-shaped diaphragm**

I. INTRODUCTION

Microelectromechanical Systems (MEMS) technology has been explored to fabricate miniature acoustic transducers on silicon wafer in order to take full advantages of MEMS (e.g., small size and weight, potentially low cost due to the batch processing, possibility of integrating transducers and circuits on a single chip, lack of transducer "ringing" due to small diaphragm mass, and etc.) [1,2,3]. These advantages make the micromachined acoustic transducers (such as microphone, microspeaker, and ultrasonic transducers) attractive in the following applications: personal communication systems, multimedia systems, hearing aids, smart sensor systems [4,5,6]. However, there are only few MEMS acoustic transducers that are currently in the process of being commercialized. This is because it is difficult to control the residual stress of the diaphragm used in MEMS acoustic transducers.

To reduce the residual stress, a dome-shaped diaphragm has been investigated in this work. The advantages of a dome-shaped diaphragm are as follows. First, a dome-shaped diaphragm is capable of releasing the residual stress in the diaphragm by itself through volumetric change of its shape, and can easily be wrinkle-free (even under a compressive residual stress) and crack-free (even under a tensile stress). Secondly, a dome diaphragm is effective in converting in-plane strain to radial diaphragm deflection, and in producing sound output. Thirdly, a dome diaphragm increases the figure of merit (the product of the fundamental resonant frequency squared and the dc response) because the dome structure with its spatial curvature is stronger and stiffer than other structural forms of the same overall dimensions and weight.

For obtaining good performance of micromachined acoustic transducers (made on a micromachined diaphragm), it is important to understand and model the mechanical behavior of the diaphragm structures. Finite Element Analysis (FEA) with ANSYS 5.6 has been performed to analyze the micromachined dome shaped diaphragm piezoelectric acoustic transducers. Structural (stress and strain) and dynamic (modal) analyses have been completed for agiven pressure load over some specific frequency ranges. Also, piezoelectric coupled field analysis has been performed to analyze coupling between the electrical and the mechanical displacement field by introducing appropriate piezoelectric matrices into

Manuscript received January 5, 2005; revised March 10, 2005
*Packaging Technology Group, National Semiconductor, Santa Clara, CA 95051
**Department of EE-Electrophysics, University of Southern California, Los Angeles, CA 90089-0271
E-mail: eskim@usc.edu

the ANSYS batch model. This paper describes the finite element analyses (FEA) with ANSYS 5.6.

II. MODELING

1. Dimension and Simplification

The geometrical dimensions of the dome-shaped diaphragm are defined with respect to the cross-sectional view of the acoustic transducer shown in Figure 1[1]. Good sphericity of a dome-shaped cavity can be obtained with the fabrication technique described in [7], though the center of the sphere is not along the surface of the silicon substrate (i.e., the dome-shaped cavity is not hemispherical).

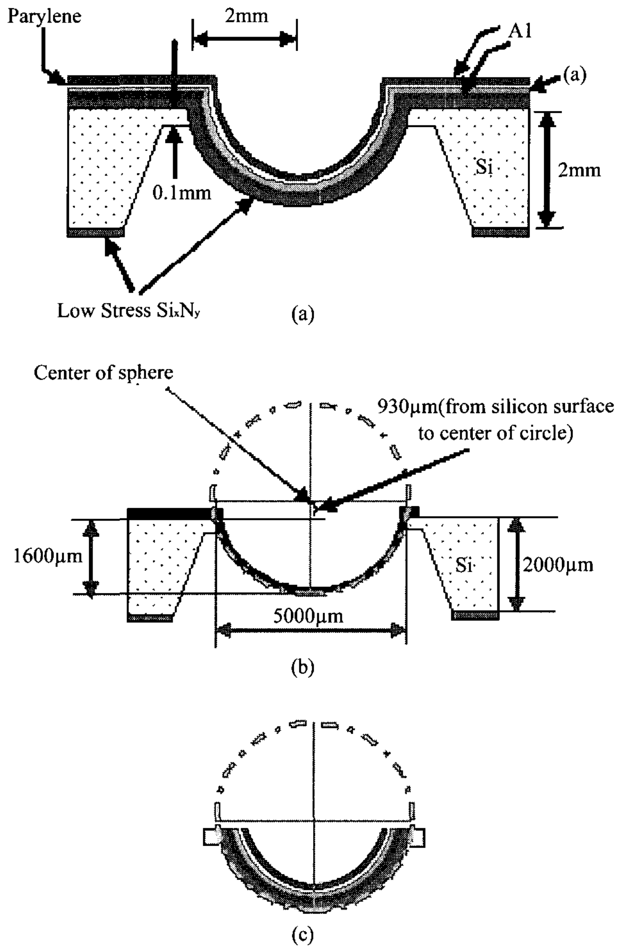

Fig. 1. (a) Cross-sectional view of the acoustic transducer. (b) The dimension of the dome-shaped diaphragm. (c) Simplified model only for diaphragm structure with fixed boundary condition

We simplify the model by ignoring the silicon substrate and modeling the dome-shaped diaphragm with a fixed boundary condition, since the vibration of the silicon substrate including the silicon rim can be ignored due to its large rigidity and thickness of the silicon substrate with respect to those of the diaphragm. Figure 1(c) shows the simplified model (i.e., the diaphragm with a fixed boundary condition).

2. Modeling Dome-Shaped Diaphragm Transducers

Due to the 3 dimensional nature of the dome-shaped diaphragm, the 3 dimensional modeling has been done. The element type of SOLID 185 (that uses eight nodes having three degree of freedom at each node) is used for modeling the mechanical layers such as aluminum, parylene, and silicon nitride film layers, while the piezoelectric ZnO layer in dome-shaped diaphragm is modeled with SOLID 5, a 3-dimensional coupled-field solid. The SOLID 5 has a three-dimensional piezoelectric and structural field capability with limited coupling between the fields. The element has eight nodes with up to six degrees of freedom at each node [ANSYS 5.6].

Table. 1. Material properties used in ANSYS analyses

Material	Thickness [μm]	Material Properties (Young's Modulus, Poisson's Ratio, Density)
Al	0.5	E=69Gpa, 0.33, 2700kg/m^3
Parylene	0.2, 1	E=3.2 GPa, 0.4, 1289 kg/m^3
ZnO	0.5	C11=210 GPa, C12=120 GPa, C13=105 GPa, C33=210 GPa, C44=43 GPa, d=5700 kg/m^3
Six Ny	0.5	E=272 GPa, 0.25, 3100 kg/m^3

For building the finite element model for dome-shaped diaphragm, direct (manual) modeling method is used instead of solid (automatic) modeling because of the high aspect ratio of the micromachined thin film structures (e.g., for aluminum electrode layer, the aspect ratio is 12,000, since the thickness = 0.5um, while the length = about 6 mm). The polarization direction of the piezoelectric ZnO is assumed to be normal to the dome surface by making the z-direction of the local coordinate system normal to the surface of dome.

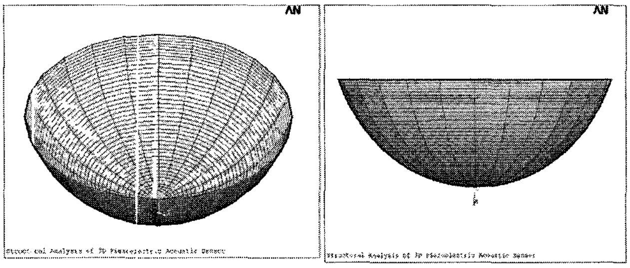

Fig. 2. Isometric and side view of the completed model for dome-shaped diaphragm acoustic transducers

By doing this, the electrodes that are deposited on the top and bottom of the ZnO layer are taken to be orthogonal to the polarization axis. This is important to get the symmetric results of the stress distribution when the piezoelectric coupled-filed analysis is done with a voltage load.

Table 1 lists the material properties (used for modeling), which are obtained from literatures. Figure 2 shows isometric and side view of the completed 3-dimensional model for the dome shaped diaphragm structure.

III. STRUCTURAL ANALYSIS

1. For 1 Pa Pressure Load

Static analysis is performed to obtain the stress distribution in the dome-shaped diaphragm with a circular clamped boundary condition, when 1 Pa pressure load is applied normal to the diaphragm surface. Figure 3 shows the isometric view and the side view of the deformed diaphragm shape. The deformed shaped is uniform except near the circular bound area, and the curvature of the deflection shape is uniform over the diaphragm. Figure 4 shows the ANSYS Von Mises stress contour plots for the diaphragm layers. The numerical values on each plot are the internal film stresses generated in the uniform stress areas. As we expect from the uniformly deformed shape in Fig. 15, the stress distribution in each film is uniform over most of the diaphragm area except near the boundary. According to Hook's law, we see stiffer layers having larger stresses for a given strain under a diaphragm deflection. Note that the stress is of the same sign (either tensile or compressive) in the diaphragm thickness direction, unlike a flat diaphragm exhibiting different signs of stress above and below the neutral plane.

2. For Voltage Load

The static coupled-field analysis (between electric and elastic field) for a piezoelectric dome-shaped-diaphragm transducer has been performed with SOLID 5 (a 3 dimensional coupled-field solid). And we have simulated the amount of stress and its distribution when a voltage

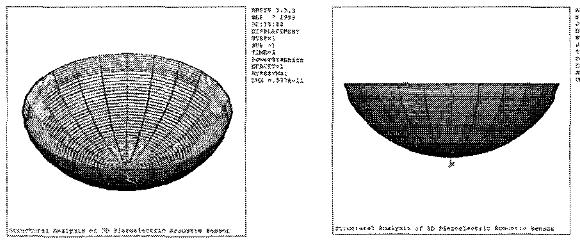

(a) (b)

Fig. 3. Isometric and side view of the deformed shape for the dome-shaped diaphragm when the 1Pa pressure load is applied. Deformed shaped is pretty uniform except near the circular bound area and the curvature over the diaphragm area is not changed

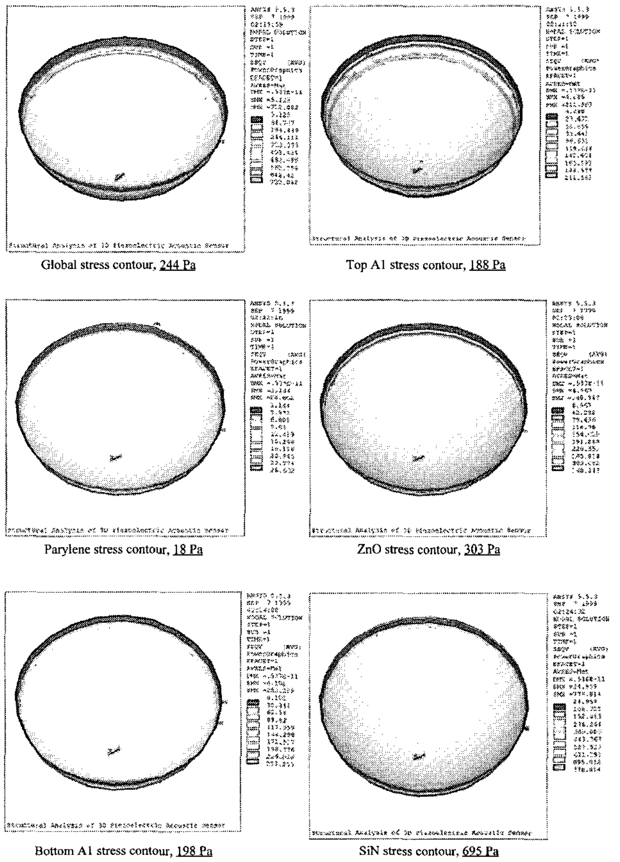

Fig. 4. ANSYS Von Mises stress contour plot for each film induced by 1Pa pressure load on top surface of the dome-shaped diaphragm. The value under each plot show the internal film stress generated in uniform stress area of dome diaphragm

load (16V on the top electrode and 0V on the bottom electrode) is applied.

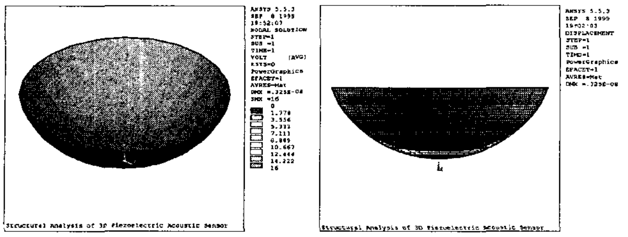

(a) (b)

Fig. 5. (a) 16V (scaled with red color) and 0V (scaled with blue color) are applied on top and bottom of the ZnO layer. (b) Deformed shape with the voltage load across the piezoelectric ZnO layer

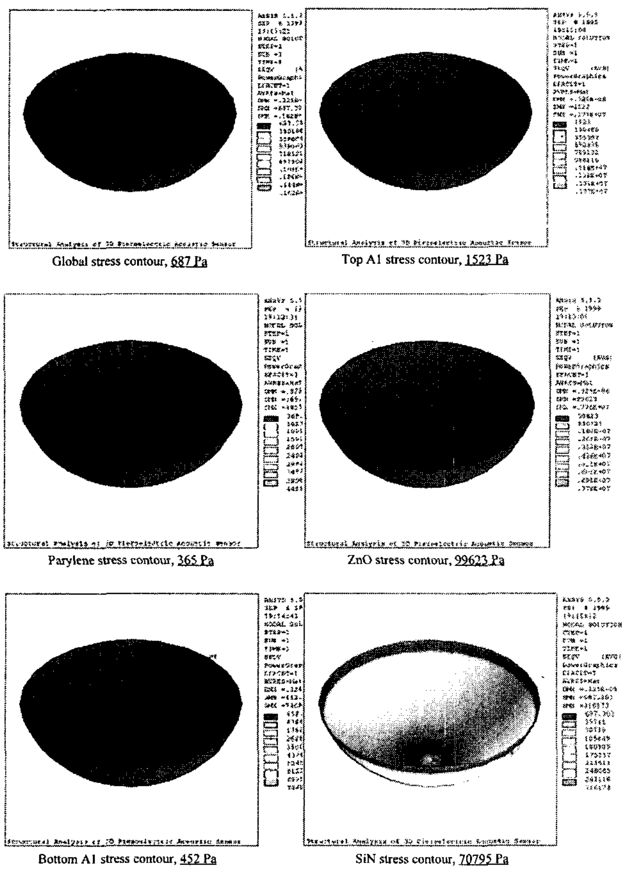

Fig. 6. ANSYS Von Mises stress contour plot for each film when the voltage load (16V on top and 0V on bottom electrode) is applied. The value under each plot show the internal film stress generated in each film on the dome-shaped diaphragm. The major stress is generated in piezo ZnO films

As can be seen in Fig. 5, the dome diaphragm is deformed almost uniformly without a curvature change. Figure 6 shows the ANSYS Von Mises stress contour plot for each film, and shows the uniform stress distribution for each film over most of the diaphragm. We note that the maximum stress (99623 Pa) is generated in the piezoelectric ZnO layer unlike the case when a pressure load is applied (in which case, the most stiff SiN experiences the highest stress). This is because the voltage is applied across the piezoelectric ZnO layer, and generates the stress, which causes the diaphragm deflection.

IV. DYNAMIC ANALYSIS

Modal analyses have been performed on the dome-shaped diaphragm acoustic transducers to determine the dynamic vibration characteristics, such as the natural frequencies and mode shapes. The Block Lanczos method (an accurate and fast method) has been chosen to solve the eigenvalue problem. First ten vibrational modes have been extracted between 0 and 1 MHz. Figure 7 shows the typical results for the first (a) and second (b) resonant modes of the diaphragm vibration. For clarity of the mode shapes, four different views (angled-top view, front view, side view and top view) are shown. Interestingly, due to the 3 dimensional nature of the dome diaphragm, the first mode shape shows a kind of rocking (nonsymmetrical) motion at 357 kHz. In this nonsymmetrical mode, the dome-shaped diaphragm is not effective in generating sound output. Note that the first resonance happens at a relatively high frequency (in relation to the diaphragm dimension) due to the structural stiffness of a dome-shaped diaphragm. This rocking mode can be used for a directional ultrasound sensing by segmenting the top and bottom electrodes, because this mode can be stimulated by any sound directed side-way. On the other hand, the second mode shape at 382 kHz shows a vibration motion that is symmetrically up and down. And the maximum sound output is expected from the second mode.

V. ANALYSIS ON DESIGN PARAMETERS

In this section, the resonant frequency of a dome-shaped diaphragm is analyzed as a function of the dome depth (illustrated in Fig. 8) and the dome size (i.e., dome

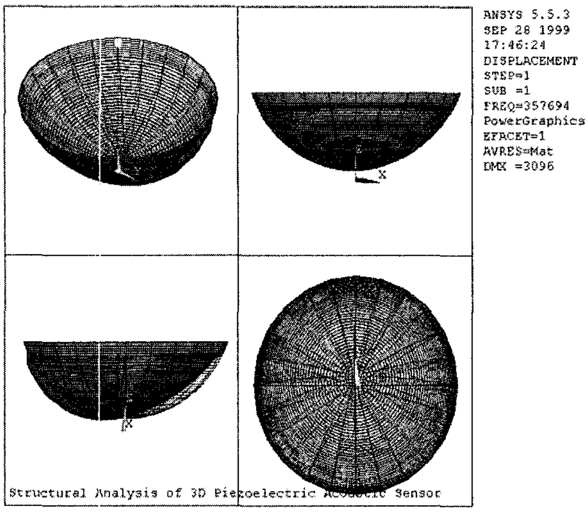

(a)

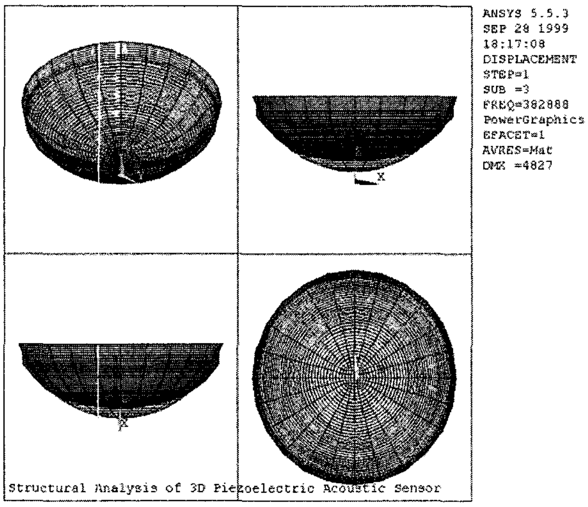

(b)

Fig. 7. Mode shapes and corresponding natural frequencies of the dome-shaped diaphragm extracted by finite element analysis using by ANSYS5.6 software. (a) First mode shows the rocking (nonsymmetrical) motion which can not generate the sound output due to the pressure compensation. (b) Second mode shows the up-and-down (symmetrical) motion which can generate the highest sound output

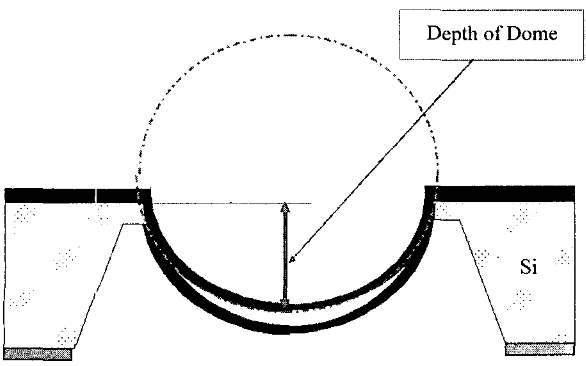

Fig. 8. Illustration for the depth of dome

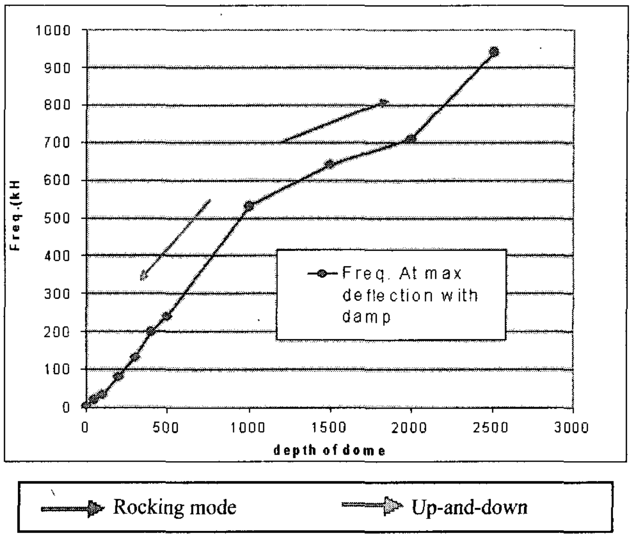

Fig. 9. The first resonance frequency as a function of the depth of dome. The first resonance frequency is getting increased when the depth of dome is increased because the structural stiffness of dome diaphragm is increase by increasing the curvature of dome

radius). Figure 9 shows the first resonant frequency as a function of the dome depth. The first resonant frequency increases with the dome depth increasing, because when the dome depth increases, the structural stiffness of a dome diaphragm increases with increasing dome curvature. This implies that a dome-shaped diaphragm is not good for a sensing purpose, since a stiff diaphragm deflects little in response to an applied pressure.

Also, it is interesting to note that there is a transition point where the mode shape of the first resonance is changed from the unsymmetrical rocking mode to the symmetrical up-and-down mode. As discussed, the mode shape of the first resonance is unsymmetrical and rocking. But as the dome depth decreases (i.e., as the dome diaphragm becomes flatter), the first rocking mode disappears and the symmetrical up-and-down mode becomes the first resonant mode. This transition has been observed when the dome depth becomes less than 1,000 μm as shown in Fig. 9. The maximum deflection amplitude at the resonant frequency also shows such an abrupt transition as can be seen in Fig. 10 (a), with the rocking mode becoming the first resonant mode as the dome depth increase beyond 1,000 μm.

When the acoustic transducer is designed for microphone or microspeaker applications, it is important to make the first resonant frequency out of the audio frequency range (i.e., beyond at least 4 kHz). Not only the

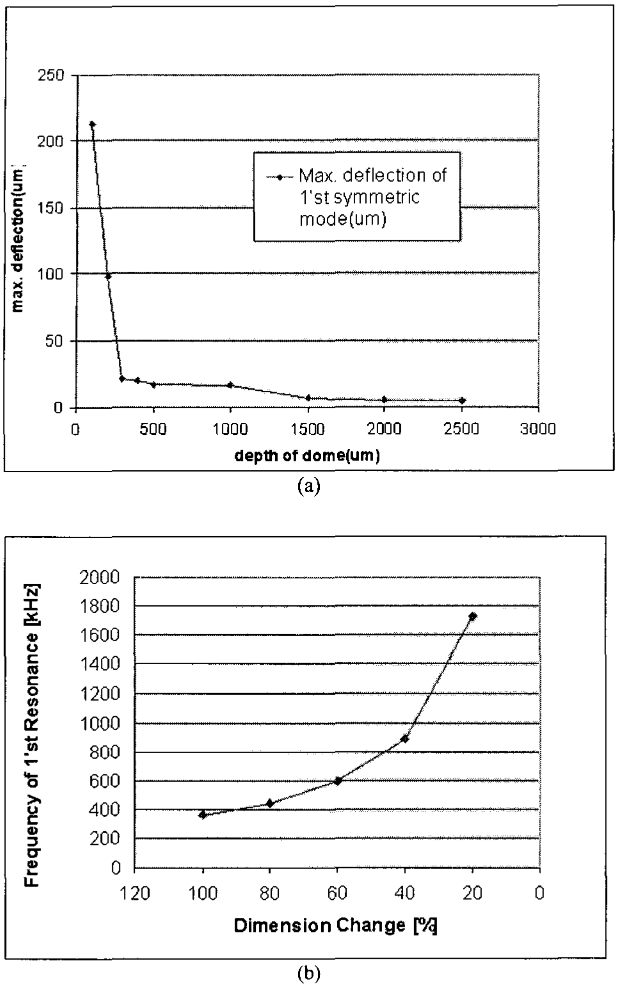

Fig. 10. (a) The maximum deflection amplitude at the frequency of first symmetric mode as a function of depth of dome for the dynamic pressure load. (b) First resonance frequency as a function of the size (diameter) of dome-shaped diaphragm

dome depth but also the dome size influences the resonant characteristics. Figure 10 (b) shows the first resonant frequency as a function of the dome size, and we see that as the diameter of a dome-shaped diaphragm decreases, the first resonant frequency increases, as expected.

VI. SUMMARY & CONCLUSIONS

Dome-shaped-diaphragm piezoelectric acoustic transducers built on a 1.5μm thick silicon nitride diaphragm (2,000 μm in radius, with a circular clamped boundary on a silicon substrate) with electrodes and piezoelectric ZnO film have been analyzed with ANSYS5.6 software. Static analyses have been performed for a 1 Pa pressure load on top of the diaphragm and for a 16V-voltage load on piezoelectric ZnO layer. Modal analyses have been done over the frequency range that the devices will be experiencing in acoustic applications. Finally, the resonance frequency and the deflection amplitude of the diaphragm are investigated by varying the design parameters, such as depth and size of a dome-shaped diaphragm.

REFERENCES

[1] C. H. Han and E. S. Kim, "Fabrication of Dome-Shaped Diaphragm with Circular Clamped Boundary on Silicon Substrate," *Proceedings of the 12th IEEE International Conference on Micro Electro Mechanical Systems (MEMS'99)*, pp. 505-510, Orlando, Florida, USA, Jan. 17 - 21, 1999.

[2] C. H. Han and E. S. Kim, "Parylene-Diaphragm Piezoelectric Acoustic Transducers," *Proceedings of the 13th IEEE International Conference on Micro Electro Mechanical Systems (MEMS'2000)*, pp. 148-152, Miyazaki, Japan, Jan. 23-27, 2000.

[3] C. H. Han and E. S. Kim, "Fabrication of Piezoelectric Acoustic Transducers Built on Cantilever-like Diaphragm," *Proceedings of the 14th IEEE International Conference on Micro Electro Mechanical Systems (MEMS'2001)*, Interlaken, Switzerland, pp. 110-113, Jan. 21-25, 2001.

[4] E. S. Kim and R. S. Muller, "IC-Processed Piezoelectric Microphone," *IEEE Electron Device Letters*, Vol. EDL-8, No. 10, pp. 467-468, Oct. 1987.

[5] W. Kuhnel and G. Hess, "Micromachined subminiature condenser microphones in silicon," *Sensors and Actuators*, A 32, pp. 560-564, 1992.

[6] G. M. Sessler, "Silicon Microphones" *J. Audio Eng. Soc.*, Vol. 44, No. 1/2, pp. 16-21, Jan. 1996.

[7] C. H. Han and E. S. Kim, "Study of Self-Limiting Etching Behavior in Wet Isotropic Etching of Silicon," *Jpn. J. Appl. Phys.* Vol. 37, pp. 6939-6941, 1998.

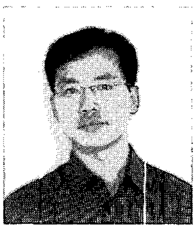

Cheol-Hyun Han He received the B.S.degree in Physics from Sungkyunkwan University in 1991. He worked at analysis and evaluation technology center at Samsung Electronics Semiconductor business as an assistant manager from 1990 to 1996. He achieved M.S. and Ph.D. degrees in electrical engineering from the University of Hawaii in 1998 and 2000, respectively. He joined Agilent Technology from 2001 to 2002 as a product development engineer in FBAR (film bulk acoustic resonator) busin ess. Currently, he works at National Semiconductor as a senior packaging development engineer from 2002. His research interests include acoustic MEMS transducers, FBAR filter, RFID, and wafer level packaging for IC and MEMS.

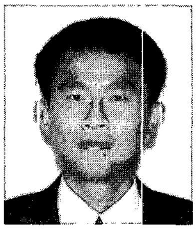

Eun Sok Kim He received the B.S. (high honors), M.S., and Ph.D. degrees, all in electrical engineering, from the University of California, Berkeley, in 1982, 1987, and 1990, respectively. His doctoral dissertation was on the integrated microphone with LSI CMOS on a single chip. In Fall 1999, he joined the University of Southern California, Los Angeles, CA, and is currently an Associate Professor in the Department of Electrical Engineering. His research interests include microelectromechanical systems (MEMS), acoustic and piezoelectric transducers, microfluidic systems, microfabrication processing technology, and materials study. From Spring 1991 to Fall 1999, he worked at the Department of Electrical Engineering in the University of Hawaii at Manoa as a faculty member. Previously, he worked at IBM Research Laboratory, San Jose, CA, NCR Corp., San Diego, CA, and Xicor Inc., Milpitas, CA as a co-op student, design engineer, and summer-student engineer, respectively. Dr. Kim serves on the editorial board for Journal of Micromechanics and Microengineering. He has been awarded a Research Initiation Award (FY 91-93) and a Faculty Early Career Development (CAREER) Award (FY 95-99) by National Science Foundation. He received Outstanding EE Faculty of the Year Award (voted by UH IEEE student chapter) in May 1996.